INTRAOSSEOUS TRANSCUTANEOUS AMPUTATION PROSTHESES *VERSUS* DENTAL IMPLANTS: A COMPARISON BETWEEN KERATINOCYTE AND GINGIVAL EPITHELIAL CELL ADHESION *IN VITRO*

C.J. Pendegrass[*], H.T. Lancashire, C. Fontaine, G. Chan, P. Hosseini and G.W. Blunn

University College London, The Institute or Orthopaedics & Musculoskeletal Science,
Centre for Biomedical Engineering, The RNOH, Brockley Hill, Stanmore, Middlesex, HA7 4LP, UK

Abstract

Infection is the primary failure modality for transcutaneous implants because the skin breach provides a route for pathogens to enter the body. Intraosseous transcutaneous amputation prostheses (ITAP) are being developed to overcome this problem by creating a seal at the skin-implant interface. Oral gingival epithelial cell attachment creates an infection-free seal around dental implants. However, this has yet to be achieved consistently outside of the oral environment. Epithelial cells attach to metal substrates by means of hemidesmosomes and focal adhesions. Their density *per* unit cell is an indicator of attachment strength. We postulate that gingival epithelial cells express more hemidesmosomes and focal adhesions at earlier time points, compared with epidermal keratinocytes, and this increased speed and strength of attachment may be the reason why an infection-free seal is often achieved around dental implants but less frequently around ITAP. The aim of this study was to compare epidermal keratinocyte with oral gingival cell attachment on titanium alloy *in vitro*, to determine whether these two cell types differ in their speed and strength of attachment. We aimed to test the hypothesis that gingival cells up-regulate focal adhesion and hemidesmosome formation at earlier time points compared with extra-oral keratinocytes. To test this hypothesis we cultured epidermal keratinocytes and oral gingival cells on titanium alloy substrates and assessed cell attachment by focal adhesions and hemidesmosome expression at 4, 24, 48 and 72 hours. Formation and expression of hemidesmosomes temporally lagged behind that of focal adhesions in both cell types. Gingival derived cells up-regulated focal adhesion and hemidesmosome expression at earlier time points compared with epidermal keratinocytes. Hemidesmosome expression in oral gingival cells was 3 times greater compared with epidermal keratinocytes at 4 hours. Our findings indicate that earlier attachment may be key to the success of the dental implant transcutaneous interface.

Keywords: *Gingival cell, epithelial cell, cell attachment, focal adhesion, hemidesmosome, laminin.*

*Address for correspondence:
Catherine Pendegrass
Centre for Biomedical Engineering
Institute of Orthopaedics and Musculoskeletal Science
University College London, Stanmore, UK
Telephone number: +44 2089 540268
E-mail: c.pendegrass@ucl.ac.uk

Introduction

Dental implants, pioneered by Brånemark, have been used successfully to treat edentulous patients since the 1960s (Adell *et al*., 1970; Marks *et al*., 2001; Odman *et al*., 1988). They have been shown to be safe and reliable, with survival rates of over 90 % at 15 years (Adell *et al*., 1986; Brånemark *et al*., 1982; Tillander *et al*., 2010). Their success relies on osteointegration and the attachment of the gingiva to the implant, which occurs through a junctional epithelium (JE) (Raisanen *et al*., 2000). The epithelial cells form a tight collar around the implant, as they do around teeth, with hemidesmosomes connecting the bordering epithelial cells of the JE, by a basal lamina-like extracellular matrix termed the internal basal lamina (IBL), to the titanium (Fig. 1). This prevents downgrowth, often termed marsupialisation or pocket formation. In downgrowth, the epidermal tissues grow down around the implant, separating it from the surrounding tissues, causing mechanical instability (Hansson *et al*., 1983). The pocket that is formed allows bacterial colonisation leading to an increased risk of infection. Translation of dental implant technology into a solution for attaching artificial limbs for amputees, could overcome the problems associated with traditional stump-socket devices, which include tissue necrosis, poor socket fitting, pain and functional impairment (Dudek *et al*., 2005; Lyon *et al*., 2000). However, despite common design concepts, skin-penetrating transcutaneous implants used for attachment of artificial limbs have been reported to have much higher infection rates compared with dental implants; with infectious complications
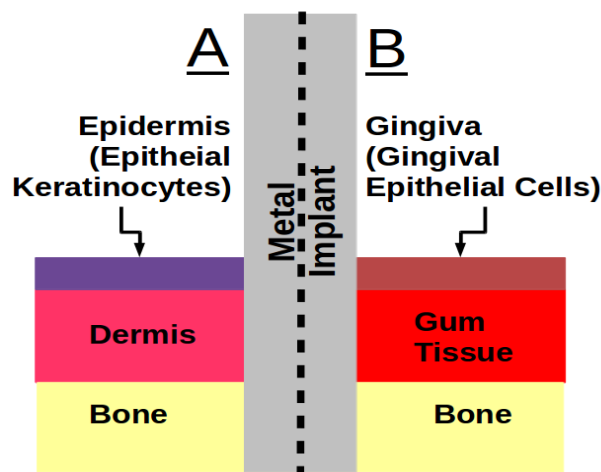

Fig. 1. Schematic demonstrating the soft tissue interface around ITAP (**A**) and a dental implant (**B**).

being reported in 40 % of patients during the first 3 years post-operation (Tillander *et al.*, 2010). Infection occurs because of downgrowth caused by failure of the epithelial cells to form a seal at the skin-implant interface, which prevents bacterial infection (Pendegrass *et al.*, 2006a). Intraosseous transcutaneous amputation prostheses (ITAP) are being developed to overcome these problems by promoting soft tissue attachment at the epithelial-implant interface, which is capable of preventing infection long-term (Middleton *et al.*, 2007; Pendegrass *et al.*, 2006b; Pendegrass *et al.*, 2008; Pendegrass *et al.*, 2010). A schematic, showing the ITAP concept, is shown in Fig. 1.

In order to prevent downgrowth, attachment of the cells in the epidermis to the implant surface is critical in order to prevent their migration, and subsequent infection. The success of dental implants may be due to earlier attachment of gingival epithelial cells, by hemidesmosomes and their pre-cursors; focal contacts, to the implant surface compared with extra-oral keratinocytes around skin-penetrating amputation prosthetics. If this is true, implant material-engineering and augmentation strategies to encourage earlier attachment of keratinocytes may reduce downgrowth and infection rates in ITAP. Hemidesmosomes facilitate stable adhesion of epithelial cells to the underlying basement membrane. Hemidesmosome stability relies on multiple interactions with a number of protein components that form a complex that is tightly embedded in the membrane (Walko *et al.*, 2014). The core of this complex is the α6β4 integrin, which binds to the extracellular matrix protein laminin-332 (laminin α3, β3, γ2 – previously termed laminin 5 (Aumailley *et al.,* 2005)). To further our understand the reasons for the poorer skin barrier created around transcutaneous devices compared with gingival mucosa around dental implants, we aim to test the hypothesis that gingival cells up-regulate focal adhesion and hemidesmosome formation at earlier time points compared with extra-oral keratinocytes, and that this may be facilitated by differences in laminin-332 expression.

Materials and Methods

Substrate preparation

10 mm diameter titanium alloy (Ti_6V_4Al) discs were manufactured from surgical grade titanium alloy (BS7252PT3). The discs were polished using successive mechanical polishing with P1200 to P4000 grade polishing paper and Buehler Micropolish 1.0 µm alumina (Buehler, Coventry UK) on and Exact-Micro-Grinding system (Mederex, Bath, UK). The surface finish on the discs measured 0.03 µm Ra. Discs were sterilised by autoclaving in a 2100 Classic Clinical Autoclave (Prestige Medical, Lancs, England) for 11 min at 126 °C and 140 kPa pressure.

Study design

The study was performed in three parts. The cells used in experiment one were human, un-matched cells (*i.e.* not from the same donor). The speed and strength of attachment of un-matched human oral keratinocytes were compared with that of extra oral keratinocytes. In experiment two, in order to determine whether the results for the un-matched human cells would be consistent with those from matched donors, primary ovine gingival and extra-oral keratinocytes were harvested, culture expanded and subjected to identical assays. In experiment three, a qualitative assessment of laminin-332 expression was performed on human un-matched cells (used in experiment one) to determine the abundance and distribution of the ECM peptide and its influence on the speed and strength of cell attachment. All assays were performed in triplicate and on the substrate materials prepared as described below.

Cell culture and seeding

Attachment of human oral gingival cells and epidermal keratinocytes
Primary human oral gingival epithelial cells (HGEP) (CellNTec, Buckingham, UK) were culture expanded in CnT24 Progenitor Cell Targeted (PCT) oral epithelium medium and supplements A, B and C (CellNTec, Buckingham, UK) with 1 % penicillin /streptomycin (Invitrogen, Corporation, Paisley, UK) at 37 °C with 5 % humidified CO_2. Primary human epidermal keratinocytes (HPEK) (CellNTec, Buckingham, UK) were culture expanded in CNT57 PCT epidermal keratinocyte medium, with identical supplements as the HGEP. 30,000 cells, at passage 1-3, were seeded on to the titanium alloy discs and cultured at 37 °C with 5 % humidified CO_2 for 4, 24, 48 and 72 h prior to assessment of cell attachment.

Attachment of ovine oral gingival cells and epidermal keratinocytes

Primary cells oral and extra oral keratinocytes were isolated from five sheep, immediately following euthanasia. Under aseptic conditions, two 10 × 20 mm biopsies were taken from both the upper gum (above the teeth) and the skin between the abdomen and thigh. Primary ovine oral gingival epithelial cells (OGEP) and primary ovine epidermal keratinocytes (OPEK) were isolated from five sheep, immediately following euthanasia. Under aseptic conditions, two 10 × 20 mm biopsies were taken from both the upper gum (above the teeth) and the skin between the abdomen and thigh. The gingival (OGEP) and extra-oral samples (OKEP) were placed in 5 mL CNT 32 PCT media and CNT 02 Non-PCT media (CellNTec, Buckingham, UK), respectively. Both media were supplemented with 1 % penicillin /streptomycin (Invitrogen, UK) and 250 ng/mL Amphotericin B (Invitrogen, UK) at 4 °C. Biopsies were floated in 5 mL of 0.25 % Trypsin/EDTA (Invitrogen, UK) under aseptic conditions for 12 h at 4 °C. The epidermis was gently scraped from the dermis with a sterile scalpel blade prior to magnetic stirring in 0.05 % Trypsin/EDTA for 20 min and incubation at 37 °C, 5 % humidified CO_2 for a further 10 min. 10 mL of Dulbecco's Modified Eagle's Medium (DMEM) (D6429 Sigma-Aldrich, UK)

supplemented with 10 % FCS (First Link Ltd., UK) and 1 % penicillin/streptomycin, was added to neutralise the Trypsin/EDTA, prior to filtering the solution through a 70 μm mesh filter (BD Biosciences, UK). The filtrate was centrifuged for 5 min, the supernatant discarded and the pellet re-suspended in 10 mL of appropriate media for each cell type. The cells were then culture-expanded before seeding as in experiment one for 4, 24, 48 and 72 h prior to the assessment of cell attachment.

Cell attachment assays
Following seeding, cells for both experiment one and two were incubated for 4, 24, 48 or 72 h prior to immunolabelling of either vinculin, for quantification of focal contacts, or BP180 for hemidesmosomes according to the following methodologies.

Focal contact quantification and analysis
Focal contacts were visualised and quantified with immunolocalisation of vinculin. Cells were fixed for 5 min in 10 % formal saline, permeabilised with 0.05 % Triton X-100 (T8787 Sigma Aldrich, Dorset; UK) and incubated with mouse monoclonal Anti-vinculin (1:100) (V9131 Sigma-Aldrich) in PBS for 2 h. FITC conjugated anti-mouse monoclonal secondary antibodies (F2883 Sigma-Aldrich) were applied in PBS (1:200) for 1 h. Cell areas were measured using a Zeiss microscope linked to image analysis software (Axioimage version 4.4, Zeiss, Germany). Vinculin markers were counted from 15 randomly selected cells on each disc (vinculin count). Three discs were used in each experimental group. The density of vinculin markers (the number of vinculin markers, divided by the cell area) was calculated and used as a method of assessing cell attachment strength. The density of vinculin markers has previously been demonstrated to directly correlate with the direct biophysical strength of cell attachment (Pendegrass *et al.*, 2010).

Hemidesmosome quantification and analysis
Hemidesmosomes were visualised and quantified with immunolocalisation of BP180. The cells were incubated with a 50 μL droplet of 10 % goat serum for 30 min to prevent non-specific antigen binding prior to incubation with rabbit monoclonal Anti-collagen XVII (BP180) (1:100) (ab28440 Abcam Plc., Cambridge, UK) in PBS for 1 h. The primary antibody was localised with Alexa Fluor 448 anti-rabbit polyclonal antibody in PBS (1:200) (ab97047 Abcam Plc., UK) for 1 h. 15 randomly selected cells *per* disc were imaged using a Zeiss microscope linked to image analysis software (Axioimage version 4.4, Zeiss, Germany) and cell fluorescence was scored using a graded scale from 0 to 5; with 0 being no fluorescence and 5 high (Fig. 2). The scale was produced in Apple Aperture (Apple Inc., USA), with each grade having a 30 unit increase in luminance as measured using the red, green, blue (RGB) (0-256) colour values.

Scanning electron microscopy
Cell morphology was assessed using a JEOL JSM-5500LV scanning electron microscope (SEM) (10 kV), at 4, 24, 48 and 72 h (n = 3). Samples were fixed in 1.5 % glutaraldehyde in 0.1 M sodium cacodylate buffer (pH 7.2) for 24 h. Following 10 min in 0.1 M sodium cacodylate buffer, cells were stained with 1 % osmium tetroxide and 1 % tannic acid in 0.1 M sodium cacodylate. Serial dehydration in industrial methylated spirit was performed prior to transferring into ethanol and then into hexamethydisalazane (HMDS). Samples were left to dry overnight, then mounted on aluminium stubs and gold-palladium sputter-coated in an Emitech K550 (Emitech Ltd. Kent, UK).

Laminin-332 expression assay
Following seeding, cells for experiment one were incubated for 4, 24, 48 or 72 h prior to immunolabelling of laminin-332 according to the following methodology. Cells were fixed for 20 min in 10 % formal saline and incubated with a 50 μL droplet of 10 % goat serum for 30 min to prevent non-specific antigen binding. Cells were incubated for 1 h with mouse monoclonal anti-human laminin alpha 3 (laminin-5) (10 μg/mL) (MAB2144, R&D Systems, Abingdon, UK). The primary antibody was localised with Alexa Fluor 448 anti-mouse polyclonal antibody in PBS (1:200) (A-11059, Life Technologies Ltd., Paisley, UK). Cells were counter-stained with Hoechst 33258 in PBS (B2883 Sigma-Aldrich) for 10 min. Cells were imaged using a Zeiss microscope linked to image analysis
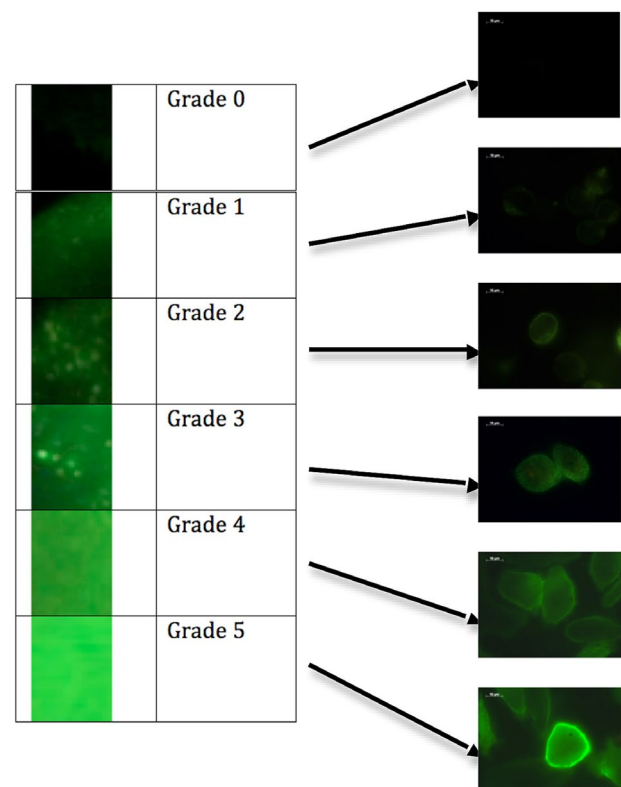

Fig. 2. Grading scale from 0-5 used to quantify the immunofluorescence for BP180 staining.
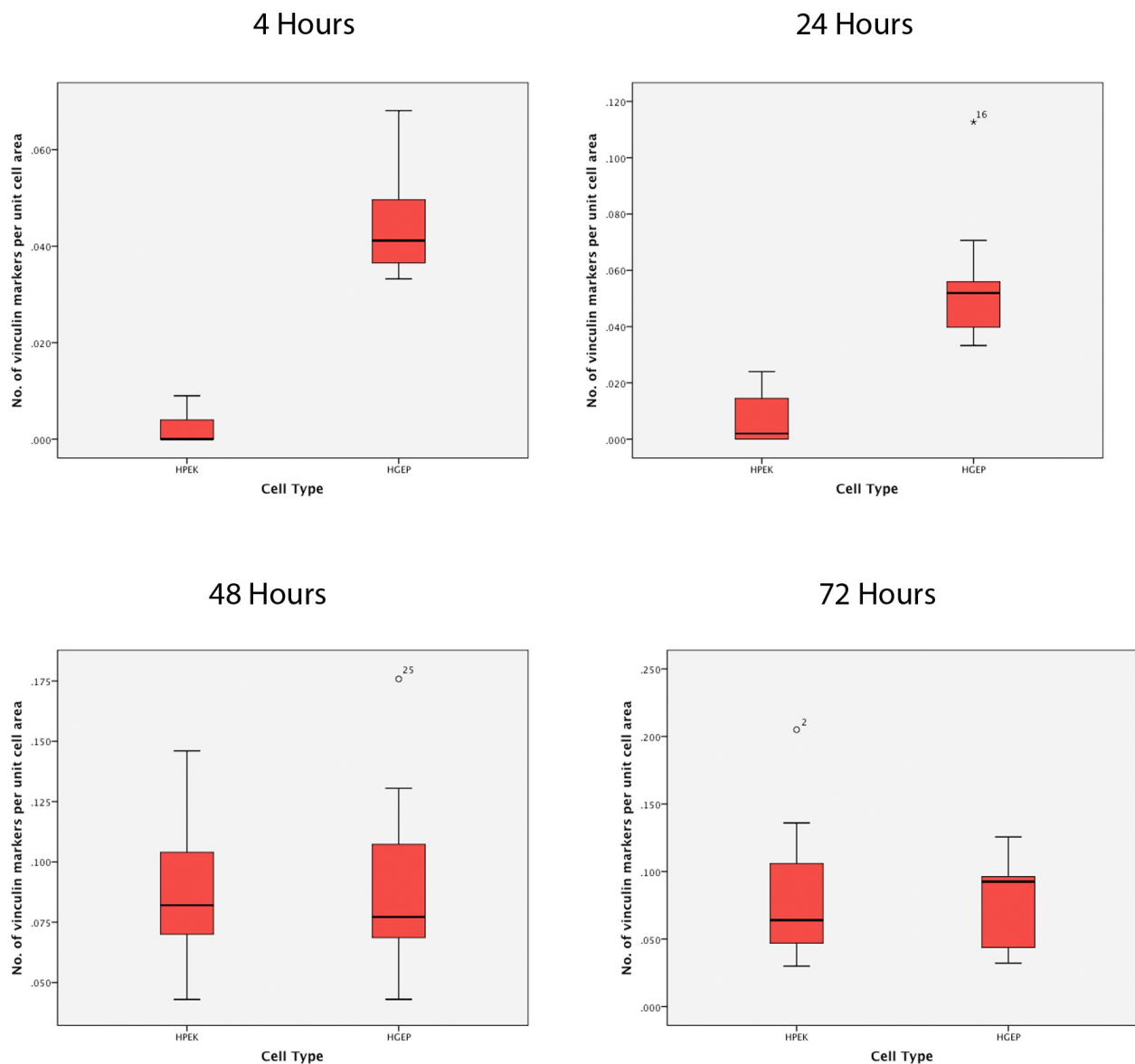
4 Hours

24 Hours

48 Hours

72 Hours

Fig. 3. Box and whiskers plots showing the number of vinculin markers *per* unit cell area for HPEK and HGEP at 4, 24, 48 and 72 h.

---

software (Axioimage version 4.4, Zeiss, Germany) and a qualitative assessment of expression was performed.

Statistical analyses

Data were analysed using SPSS (version 19.0 for windows, Chicago, USA). The Kruskal Wallis H test (KW) was used to determine whether multiple groups were from the same population distribution. If the *p* value obtained was > 0.05 the data were not subject to further analyses. Data with KW $p < 0.05$ were subject to pair-wise Mann-Whitney U (MWU) tests to assess differences between individual groups. Results were considered significant where the *p* value was less than 0.05. Data are presented as median values (with 95 % confidence intervals (CI)).

Results

Cell attachment assays: attachment of human oral gingival cells and epidermal keratinocytes

Focal contact quantification and analysis

The data are presented in Fig. 3 and Fig. 4. Significant differences in the number of vinculin markers *per* unit cell area were observed between HGEP and HPEK at 4 h ($p < 0.001$) and 24 h ($p < 0.001$). The number of vinculin markers *per* unit cell area was 15 and 7.7 times greater for the HGEP compared with the HPEK at 4 and 24 h, respectively. At 48 and 72 h, no significant differences were observed between the two cell types.

The number of vinculin markers *per* unit cell area in HPEK significantly increased between 4 and 24 h ($p = 0.037$), 24 and 48 h ($p = 0.037$), whilst HGEP only show a significant increase between 24 and 48 h ($p < 0.001$).
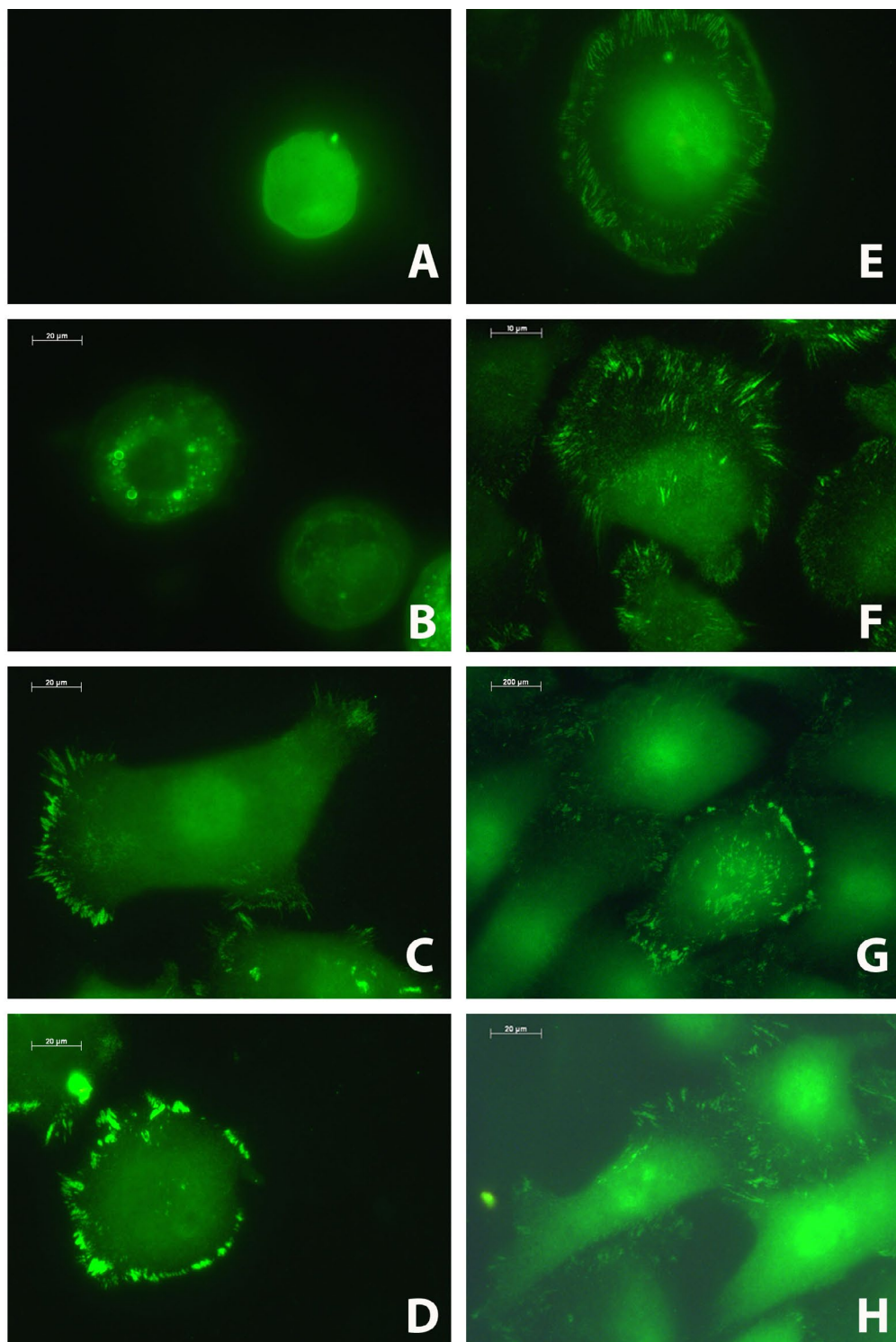
Fig. 4. Experiment one: Fluorescent microscopy images of vinculin immunolocalisation for HPEK at 4 h (**A**), 24 h (**B**), 48 h (**C**) and 72 h (**D**) and HGEP at 4 h (**E**), 24 h (**F**), 48 h (**G**) and 72 h (**H**).

Hemidesmosome quantification and analysis

It was difficult to visualise individual hemidesmosomes using light microscopy due to their small size and for this reason a score that semi-quantified the number of hemidesmosomes based on their overall fluorescence when conjugated with Anti BP180 was used. The BP180 score was significantly greater in HGEP compared with HPEK at 4 h ($p = 0.002$). No significant differences were observed at 24 ($p = 0.605$), 48 ($p = 0.436$) or 72 h ($p = 0.258$) (Table 1 and Fig. 5). Distinct differences

were noted in cell morphology between the cell types from 24 h, with HGEP adopting a more flattened, spread morphology compared with HPEK which were observed to be rounder with fewer cell processes (Fig. 5).

Over time, data analysis for each cell type showed that BP180 score significantly increased between all time-points in HPEK (p values = 0.040 (between 4 and 24 h), 0.019 (24 and 48 h) and 0.000 (48 and 72 h); however, similar increases were only observed in HGEP between 24 and 48 h ($p = 0.011$), and 48 and 72 h
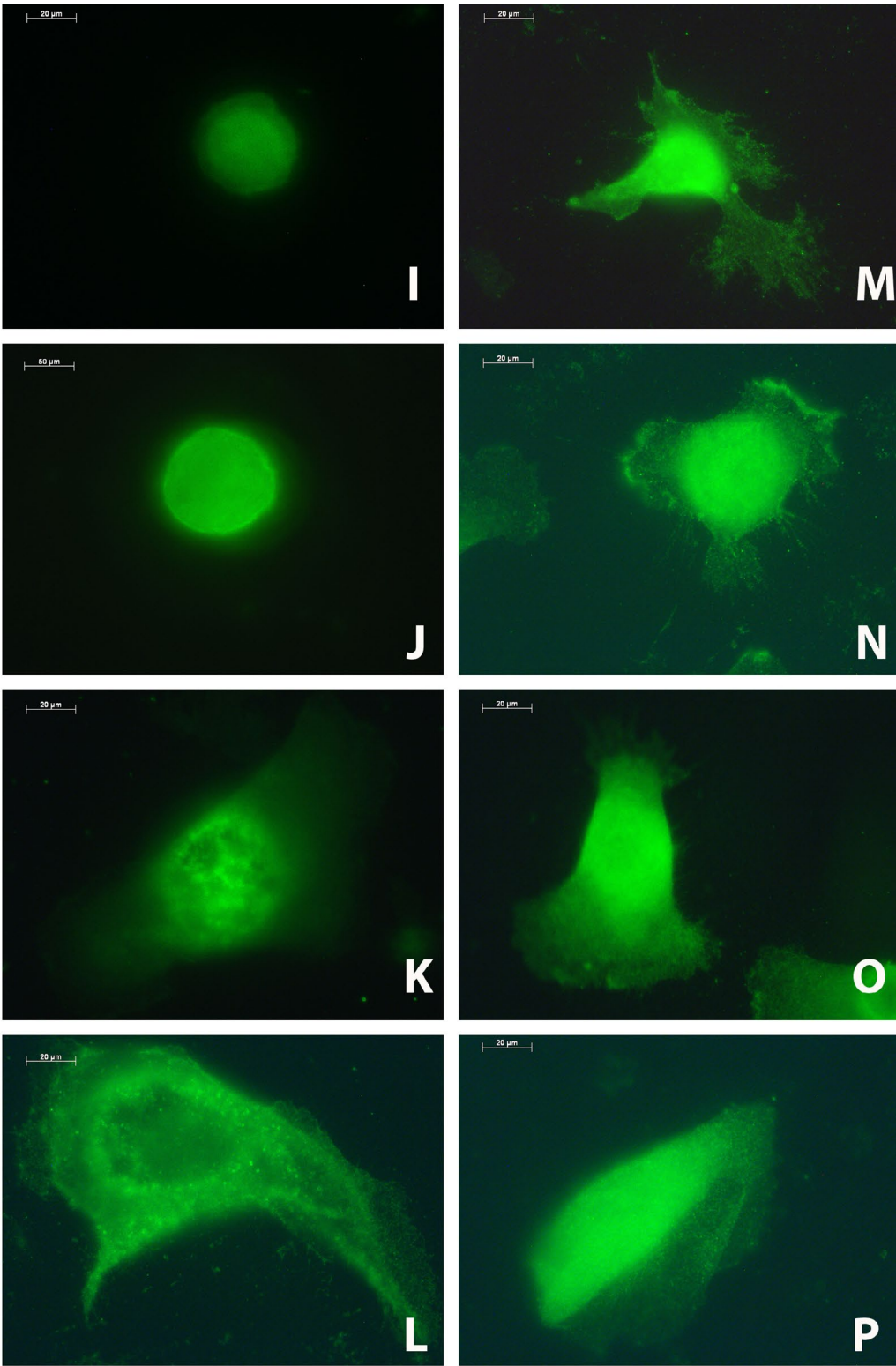
Fig. 5. Experiment one: Fluorescent microscopy images of BP180 staining for HPEK at 4 h (**I**), 24 h (**J**), 48 h (**K**) and 72 h (**L**) and HGEP at 4 h (**M**), 24 h (**N**), 48 h (**O**) and 72 h (**P**).

Table 1. Median and 95 % Confidence intervals for Experiment One BP180 scores over time for HPEK and HGEP.

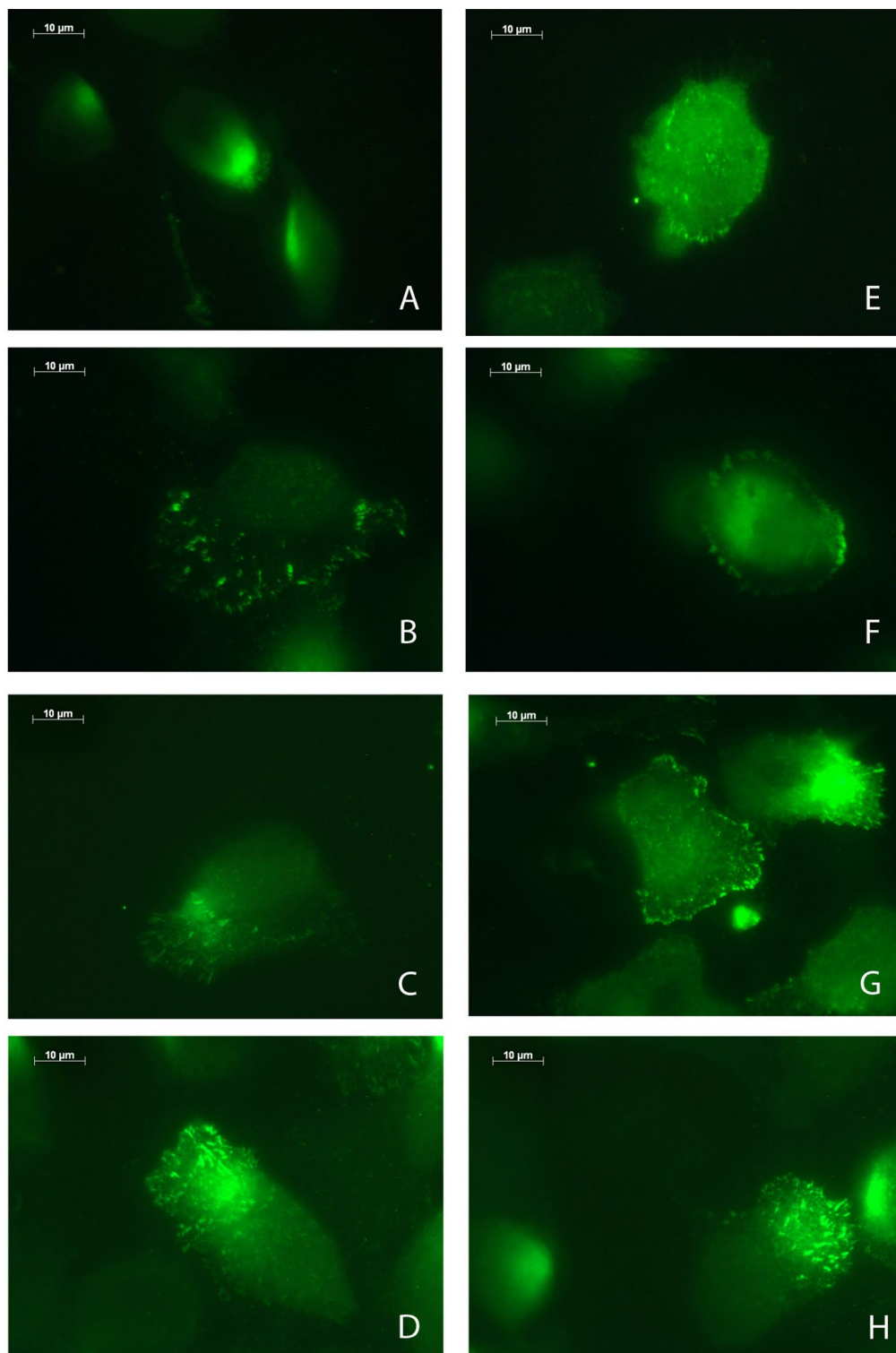| Cell Type	Time (h)			
	4	24	48	72
HPEK	2.0 (1.2 to 2.0)	2.0 (1.8 to 2.9)	3.0 (2.9 to 3.6)	5.0 (4.2 to 5.0)
HGEP	3.0 (2.3 to 3.3)	3.0 (2.2 to 3.0)	3.0 (3.0 to 3.9)	4.0 (3.9 to 5.0)

Fig. 6. Experiment two: Fluorescent microscopy images of vinculin immunolocalisation for OPEK at 4 h (**A**), 24 h (**B**), 48 h (**C**) and 72 h (**D**) and OGEP at 4 h (**E**), 24 h (**F**), 48 h (**G**) and 72 h (**H**).

(p = 0.019). No significant increase was observed in HGEP between 4 and 24 h (p = 0.546).

Cell attachment assays: attachment of ovine oral gingival cells and epidermal keratinocytes

Focal contact quantification and analysis
Significant differences in the number of vinculin markers *per* unit cell area were observed between OGEP and OPEK at 4 h (p = 0.012), 24 h (p < 0.001), 48 h (p < 0.001) and 72 h (p = 0.018) (Table 2 and Fig. 6). The density of vinculin markers was 1.3, 1.4, 1.4 and 1.2 times greater for the OGEP compared with the OPEK at 4, 24, 48 and 72 h respectively.

The density of vinculin markers in OPEK significantly increase between 4 and 24 h (p = 0.001), 24 and 48 h (p < 0.001), and 48 and 72 h (p < 0.001). Significant increases were observed for OGEP between
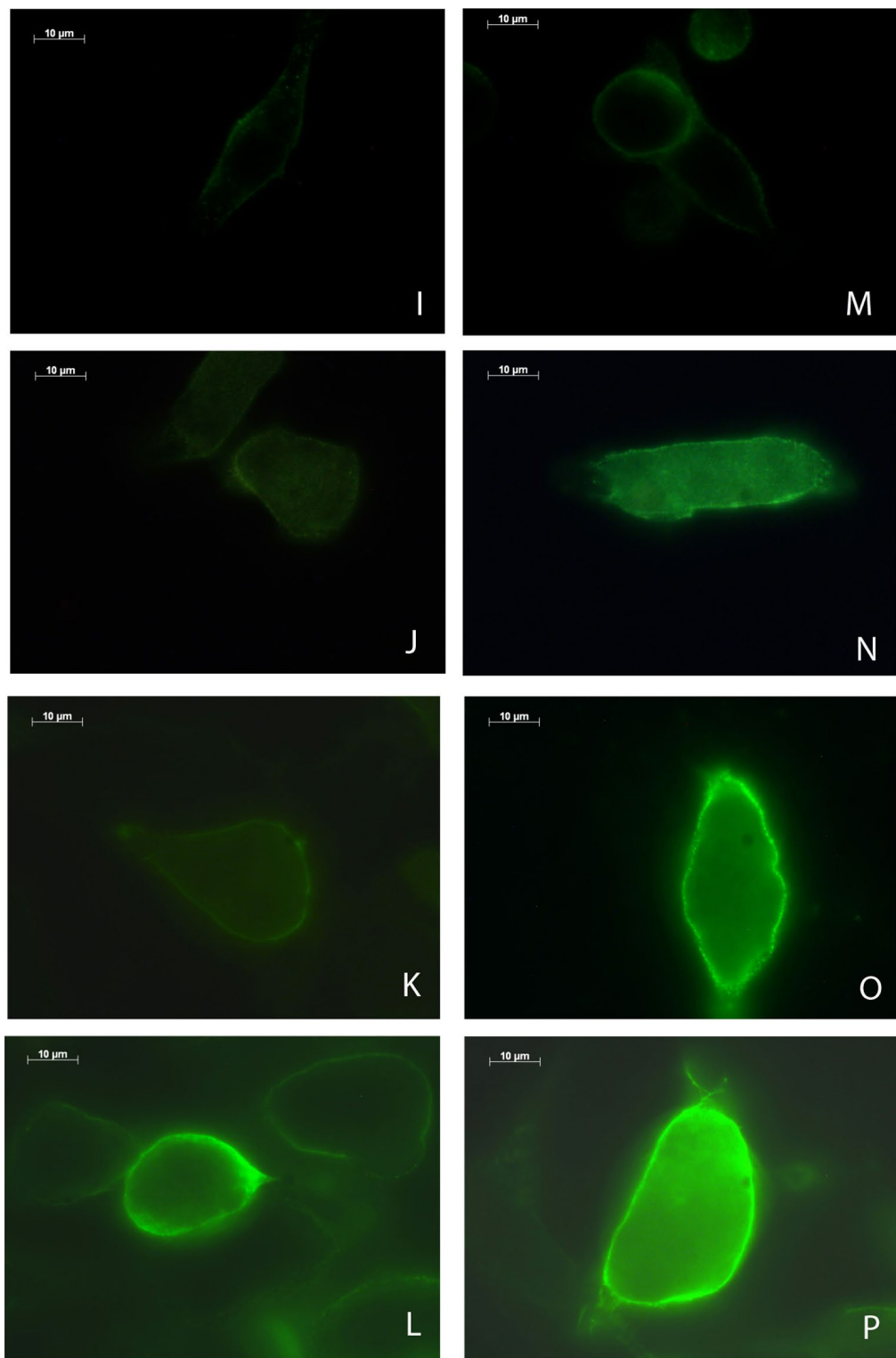
Fig. 7. Experiment two: Fluorescent microscopy images of BP180 staining for OPEK at 4 h (**I**), 24 h (**J**), 48 h (**K**) and 72 h (**L**) and OGEP at 4 h (**M**), 24 h (**N**), 48 h (**O**) and 72 h (**P**).

Table 2. Median and 95 % Confidence intervals for Experiment Two number of vinculin markers per unit cell area over time for OPEK and OGEP.

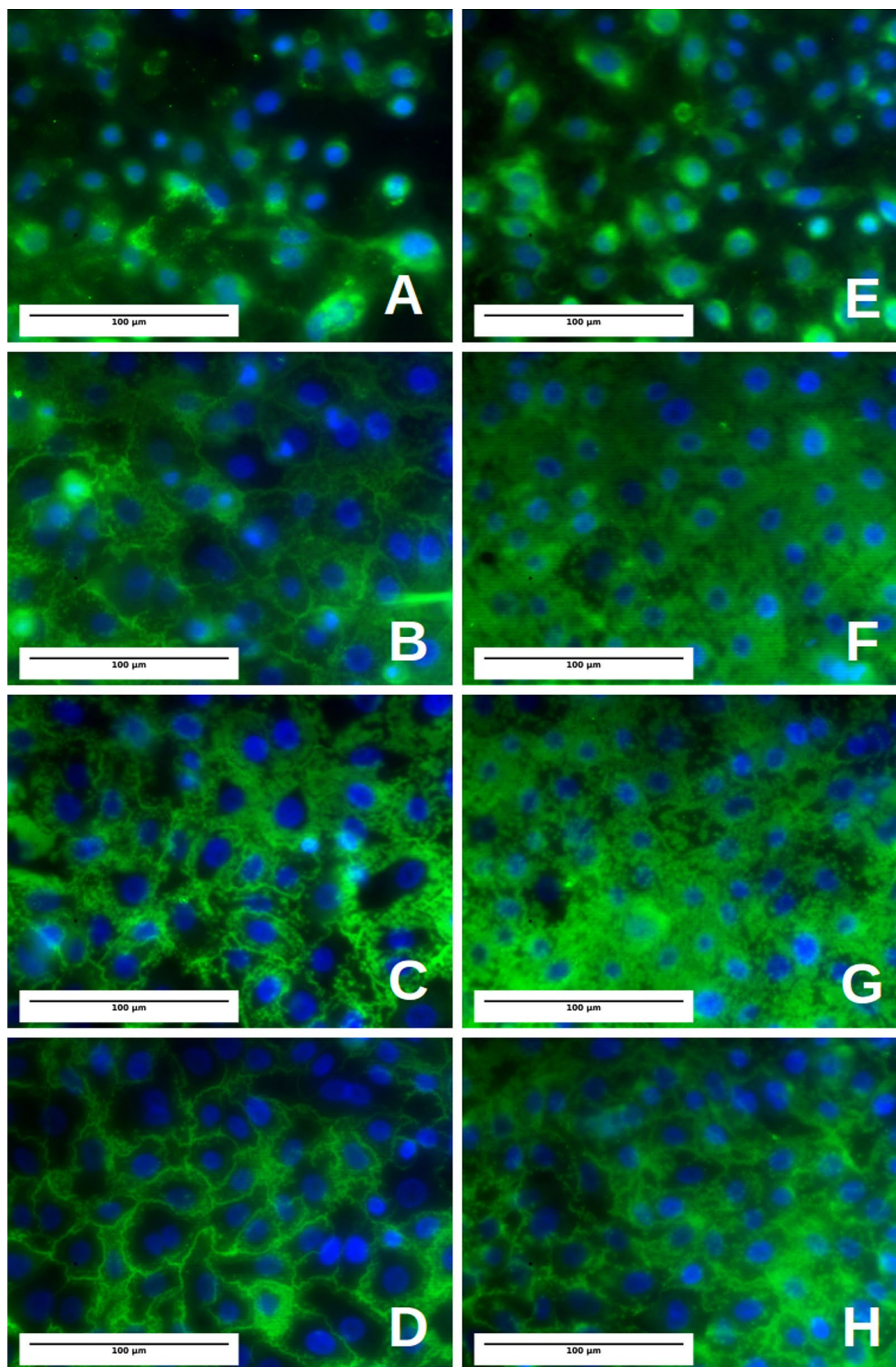| Cell Type	Time (h)			
	4	24	48	72
OPEK	0.03 (0.02 to 0.04)	0.05 (0.04 to 0.06)	0.08 (0.07 to 0.09)	0.11 (0.10 to 0.12)
OGEP	0.04 (0.04 to 0.05)	0.07 (0.07 to 0.10)	0.11 (0.11 to 0.14)	0.13 (0.12 to 0.15)

Fig. 8. Laminin-332 expression Assay: Fluorescent microscopy images of HPEK at 4 h (**A**), 24 h (**B**), 48 h (**C**) and 72 h (**D**) and HGEP at 4 h (**E**), 24 h (**F**), 48 h (**G**) and 72 h (**H**).
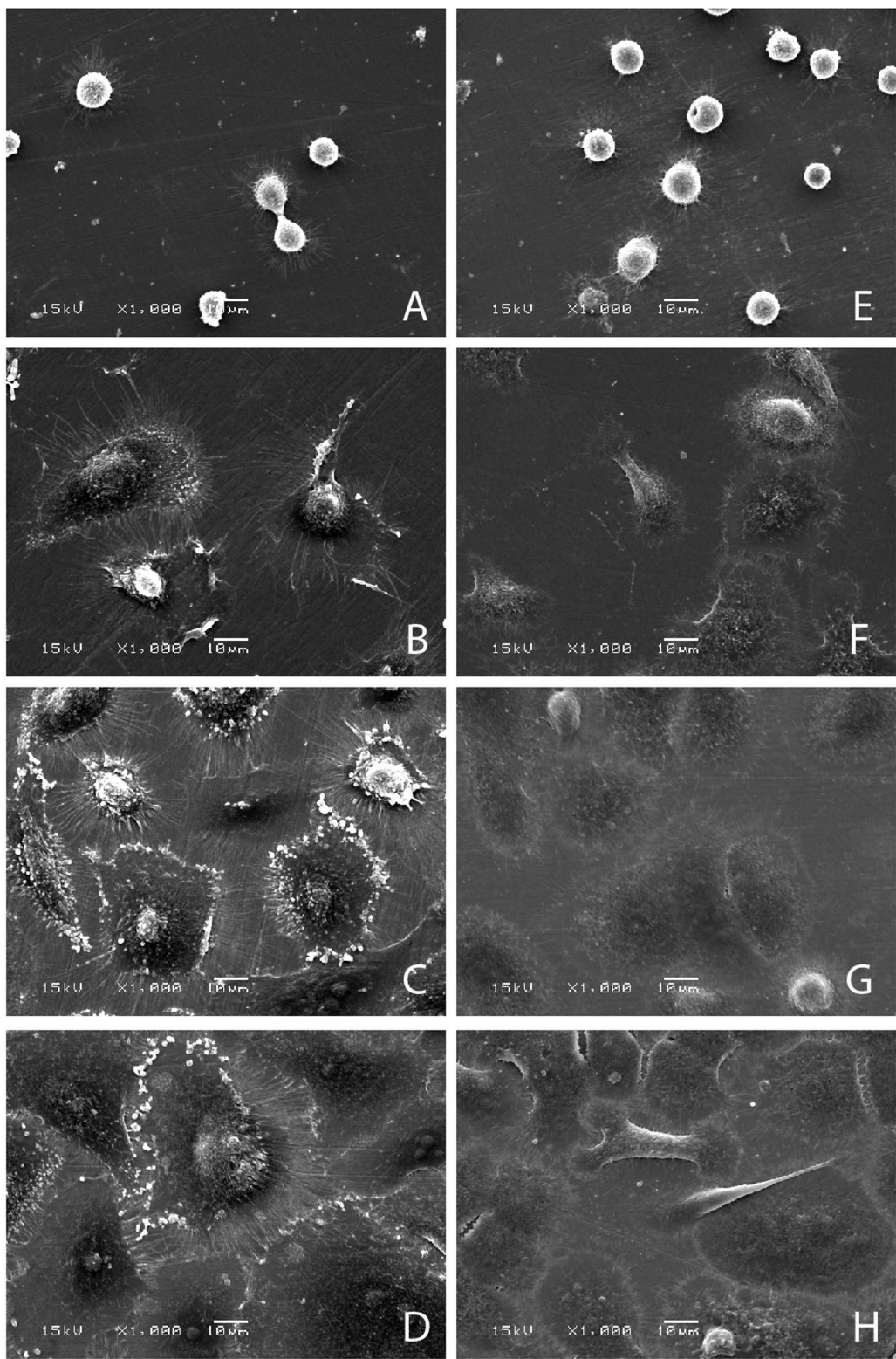
Fig. 9. Experiment two: Scanning electron microscopy images of OPEK at 4 h (**A**), 24 h (**B**), 48 h (**C**) and 72 h (**D**) and OGEP at 4 h (**E**), 24 h (**F**), 48 h (**G**) and 72 h (**H**).

Table 3. Median and 95 % Confidence intervals for Experiment Two BP180 scores over time for OPEK and OGEP.

	Time (h)			
Cell Type	**4**	**24**	**48**	**72**
OPEK	1.0 (0.6 to 1.0)	1.0 (0.9 to 1.4)	2.0 (2.2 to 2.7)	4.0 (4.0 to 4.4)
OGEP	3.0 (2.6 to 3.2)	3.0 (2.8 to 3.4)	4.0 (4.0 to 4.5)	4.0 (4.3 to 4.6)

4 and 24 h ($p < 0.001$), and between 24 and 48 h ($p < 0.001$); however, no significant increase was observed thereafter ($p = 0.226$).

Hemidesmosome quantification and analysis
The data are presented in Table 3 and Fig. 7. The BP180 score was significantly greater in OGEP compared with OPEK at 4 ($p < 0.001$), 24 ($p < 0.001$), 48 ($p < 0.001$) and 72 h ($p = 0.023$). Unlike the human cells, morphological differences were not observed between the two primary ovine cell types. The BP180 score was 3 times greater for OGEP compared with OPEK at both 4 and 24 h, and 2 times greater at 48 h.

Over time, data analyses for each cell type showed that BP180 score significantly increased between all time points in OPEK (p values = 0.033 (between 4 and 24 h), < 0.001 (24 and 48 h) and < 0.001 (48 and 72 h); however, similar significant increases were only observed in OGEP between 24 and 48 h ($p < 0.001$), and 48 and 72 h ($p < 0.001$). No significant increase was observed in OGEP between 4 and 24 h ($p = 0.344$). These findings support those for the unmatched human cell data.

Laminin-332 expression assay
The results are presented in Fig. 8. At 4 h, the abundance and localisation of laminin-322 expression appear to be similar between HPEK and HGEP, however at 24 and 48 h, expression in HGEP appears to be more abundant and distributed evenly over the surface of the substrates (both beneath and between cells). In contrast, expression in HPEK is located primarily between cells – with only limited evidence of localised expression at the cell-substrate interface at 24 and 48 h. At 72 h, laminin-332 remains more abundant in HGEP cultures, with expression observed both between cells and at the cell-substrate, whist in HPEK, the expression is almost entirely observed at the cell-cell boundaries.

Scanning electron microscopy
The data are presented in Fig. 9. At 4 h, the OGEP adopted a flatter morphology with more numerous cytoplasmic processes compared with the OPEK, typical of cells forming earlier cell-substrate attachments. By 48 h, the substrates were supporting monolayers of both cell types; however, OGEP were seen to be adopting a flatter morphology with more continuous monolayers compared with OPEK. This persisted up to 72 h.

Discussion

This is the first study to directly compare oral gingival epithelial cell and epidermal keratinocyte adhesion to titanium alloy *in vitro*. We have demonstrated that for pooled human, and matched ovine cells, oral gingival derived cells up-regulate both focal adhesion and hemidesmosome expression at earlier time points compared with epidermal keratinocytes. With pooled human cells, this up-regulation was significant for both

focal adhesion and hemidesmosome expression at 4 h, and for matched ovine cells, at all time-points.

Raisanen *et al.* showed that focal adhesions develop earlier than hemidesmosomes in epidermal keratinocytes, and this is consistent with the results of our current study (Raisanen *et al.*, 2000). Pendegrass *et al.* demonstrated that hemidesmosome and focal adhesion expression significantly increase over time for immortalised human keratinocytes cultured on titanium alloy (Pendegrass *et al.*, 2008). Our current findings substantiate this with primary pooled human and primary matched ovine epidermal keratinocytes. However, it is of note that there is no significant increase in hemidesmosome expression for gingival cells between 4 and 24 h. For pooled human and matched ovine gingival cells, the expression of BP180 was found to be 1.5 and 3 times greater than epidermal keratinocytes at 4 h. This demonstrates that the up-regulation occurred in the first 4 h of cell contact with the substrates and we postulate that this early attachment is key to the success of the transcutaneous interface observed in dental implants. Since hemidesmosomes are considered to 'enforce stable attachment of basal cells to the basement membrane in stratified epithelia' (Goldfinger *et al.*, 1999), we also propose that gingival cells attach to titanium alloy more strongly than epidermal keratinocytes and, combined with earlier adhesion, this may play a role in the success of dental implant interfaces. We have observed a greater amount and more ubiquitous distribution of laminin-332 expressed by HGEP at 24, 48 and 72 h, compared with HPEK. Since the α6β4 integrin binds with laminin-332 (Aumailley *et al.,* 2005), this is consistent with our findings for vinculin and hemidesmosome expression and supports our hypothesis. Despite this, at 4 h we did not observe a difference in either abundance or distribution of laminin-332 between cell types. It is possible that the increased hemidesmosomes expressed in HGEP cells at this time point, are not yet associated with the ECM laminin-332. Temporal transcription and translation pathways of the two lag behind one another, such that hemidesmosome expression precedes that of laminin-332. This would require further research beyond the remit of this paper. However, we also accept that additional components of the ECM, including other laminin isoforms, type IV collagen, nidogen and heparin sulphate may also play important roles in the complex process of cell attachment. There would be merit in investigating these in addition. We acknowledge that our use of titanium alloy differs from that of commercially pure titanium, which is most frequently utilised in the dental implant field, and the results seen with this surface may be different from that seen with commercially pure titanium. However, the differences were not specific to the titanium surface but rather to the type of cell. For ITAP, titanium alloy provides improved biocompatibility, higher tensile strength and improved fatigue resistance compared with commercially pure titanium, making it the material of choice for trans-femoral implants, as the implant has to sustain large loads associated with walking.

The results of this study suggest that up-regulation of epidermal keratinocyte attachment around ITAP may

enhance the skin seal. This premise is based on the fact that the problems of implant infection around dental implants are less than with transcutaneous implants and that one reason may be the relatively poor adhesion characteristics of cutaneous epidermal cells compared with gingival cells. However, we acknowledge that this may not be the only factor involved in the formation of an effective skin seal and other parameters, *e.g.* cell proliferation and migration, may also be important in the formation and maintenance of the interface *in vivo*. One of the key features of the soft tissues around the tooth and dental implant abutments is the tightly adherent nature of the soft tissues, where there is limited movement. This is in contrast to the skin, which is highly mobile and one of the key features of a successful transcutaneous implant is associated with limiting this movement. However, the adhesion of the epithelium to the implant surface is important in maintaining a long lasting functional seal.

Based on this paper, augmentation strategies to promote earlier epidermal keratinocyte attachment may prove beneficial in developing a seal at the transcutaneous interface. The attachment of the marginal gingiva to a tooth surface is mediated by the thin non-keratinised JE, which attaches to the tooth surface through hemidesmosomes and the IBL (Bosshardt *et al*., 2005; Ikeda *et al*., 2000; Masaoka *et al*., 2009; Oksonen *et al*., 2001; Shimono *et al*., 2003; Shiraiwa *et al*., 2002). The JE that develops around dental implants contains laminin-332 and is expressed by cells of the oral mucosa (Masaoka *et al.*, 2009). The oral mucosa is the site from which the gingival cells for this study were derived. The success of the transcutaneous interface around teeth and dental implants can be attributed to JE, and specifically to the α6β4 integrin component of hemidesmosomes (Masaoka *et al*., 2009; Oksonen *et al*., 2001; Shimono *et al*., 2003) and the laminin-332 component of the IBL (Ikeda *et al*., 2000; Fukano *et al*., 2006). The IBL has been shown to contain a 12-fold higher laminin-332 content compared with the rest of the JE (Kinumatsu *et al*., 2009). We hypothesised that the attachment characteristics of the cells from the two sources would have different attachment capabilities and that laminin-332 may be in part responsible for this. This we have shown the former to be correct, and there to be a distinct difference in the abundance and special distribution of laminin-332 in the cells extracellular matrices. Laminin-332 (L5); is known to bind to the α6β4 integrin of hemidesmosomes mediating cell attachment to the basal lamina of both oral and extra-oral epithelial cells and this has been shown to gradually increase over time in oral gingival epithelial cell cultures on titanium alloy (Shiraiwa *et al*., 2002) where it regulates epidermal cell migration and attachment in wound healing (Goldfinger *et al*., 1999). Based on our findings and those of others, implicating laminin-332 in enhancing human epidermal keratinocyte attachment to titanium alloy (Ikeda *et al*., 2000), it may have a role to play in improving attachment at the skin-implant interface in clinical application. Covalently attaching laminin-332 through silanisation has been shown to up-regulate vinculin cell attachment markers in keratinocytes *in vitro* (Gordon *et al*., 2010). The

consequences of attachment of laminin-332 molecules to the implant surface has been shown to be beneficial for the attachment of keratinocytes *in vitro* but the success of this for improving the skin-implant interface (*in vivo*) remains to be demonstrated.

Conclusion

This study has provided evidence that gingival derived cells up-regulate focal adhesion and hemidesmosome expression at earlier time points compared with epidermal keratinocytes when cultured on titanium alloy substrates and that laminin-332 expression may be in part responsible for these findings. Hemidesmosome expression in oral gingival cells was found to be 3× greater compared with that of epidermal keratinocytes at 4 h. This early attachment may be responsible for formation of a successful gingival-implant interface around dental implants. If strategies could be developed to promote earlier and stronger keratinocyte adhesion to the biomaterials used for extra-oral transcutaneous devices, the associated issues of downgrowth and infection may be prevented, enabling ITAP to be used clinically with an effective infection-free skin seal.

References

Adell R, Hansson BO, Branemark PI, Breine U (1970). Intraosseous anchorage of dental prostheses. II. Review of clinical approaches. Scand J Plastic Recon Surg **4**: 19-34.

Adell R, Lekholm U, Rockler B (1986). Marginal tissue reactions at osseointegrated titanium fixtures (I). A 3-year longitudinal prospective study. Int J Oral Maxfac Surg **15**: 39-52.

Aumailley M, Bruckner-Tuderman L, Carter WG, Deutzmann R, Edgar D, Ekblom P, Engel J, Engvall E, Hohenester E, Jones JC, Kleinman HK, Marinkovich MP, Martin GR, Mayer U, Meneguzzi G, Miner JH, Miyazaki K, Patarroyo M, Paulsson M, Quaranta V, Sanes JR, Sasaki T, Sekiguchi K, Sorokin LM, Talts JF, Tryggvason K, Uitto J, Virtanen I, von der Mark K, Wewer UM, Yamada Y, Yurchenco PD (2005). A simplified laminin nomenclature. Matrix Biol **24**: 326-332.

Bosshardt DD, Lang NP (2005). The junctional epithelium: from health to disease. J Dent Res **84**: 9-20.

Branemark PI, Albrektsson T (1982). Titanium implants permanently penetrating human skin. Scand J Plast Reconstr Surg **16**: 17-21.

Dudek NL, Marks MB, Marshall SC, Chardon JP (2005). Dermatologic conditions associated with use of a lower – extremity prosthesis. Arch Phys Med and Rehabil **86**: 659-663.

Fukano Y, Knowles NG, Usui ML, Underwood RA, Hauch KD, Marshall AJ, Ratner BD, Giachelli C, Carter WG, Fleckman P, Olerud JE (2006). Characterization of an *in vitro* model for evaluating the interface between skin and percutaneous biomaterials. Wound Rep Regen **14**: 484-491.

Goldfinger LE, Hopkinson SB, DeHart GW, Collawn S, Couchman JR, Jones JC (1999). The alpha-3 laminin subunit, alpha6beta4 and alpha3beta1 integrin coordinately regulate wound healing in cultured epithelial cells and in the skin. J Cell Sci **112**: 2615-2629.

Gordon DJ, Bhagawati DD, Pendegrass CJ, Middleton CA, Blunn GW. J Biomed Mater Res A **94**: 586-593.

Hansson HA, Albrektsson T, Branemark PI (1983). Structural aspects of the interface between tissue and titanium implants. J Prosthet Dent **50**: 108-113.

Ikeda H, Yamaza T, Yoshinari M, Ohsaki Y, Ayukawa Y, Kido MA, Inoue T, Shimono M, Koyano K, Tanaka T (2000). Ultrastructural and immunoelectron microscopic studies of the peri-implant epithelium-implant interface of rat maxilla. J Peridontol **71**: 961-973.

Kinumatsu T, Hashimoto S, Muramatsu T, Sasaki H, Jung HS, Yamada S, Shimono M (2009). Involvement of laminin an dintegrins in adhesion and migration of junctional epithelium cells. J Peridontal Res **44**: 13-20.

Lyon CC, Kullkarni J, Zimerson E, Van Ross E, Beck MH (2000). Skin disorders in amputees. Am Acad Dermatol **42**: 501-507.

Marks JL, Michael JW (2001). Science, medicine and the future: Artifical limbs. Br Med J **323**: 732-735.

Masaoka T, Hashimoto S, Kinumatsu T, Muramatsu T, Jung HS, Yamade S, Shimono M (2009). Immunolocalisation of laminin and integrin in regenerating junctional epithelium of mice after gingivectomy. J Periodontal Res **44**: 489-495.

Middleton CA, Pendegrass CJ, Gordon D, Jacob J, Blunn GW (2007). Fibronectin silanized titanium alloy: A bioinductive and durable coating to enhance fibroblast attachment *in vitro*. J Biomed Mater Res A **83**: 1032-1038.

Odman J, Lekholm U, Jemt T, Branemark PI, Thilander B (1988). Osseointegrated titanium implants – a new approach in orthodontic treatment. Eur J Orthod **10**: 98-105.

Oksonen J, Sorokin LM, Virtanen M, Hormia M (2001). The junctional epithelium around murine teeth differs from gingival epithelium in its basement membrane composition. J Dent Res **80**: 2093-2097.

Pendegrass CJ, Goodship AE, Blunn GW (2006a). Development of a soft tissue seal around bone anchored transcutaneous amputation prostheses. Biomaterials **27**: 4183-4191.

Pendegrass CJ, Goodship AE, Price JS, Blunn GW (2006b). Nature's answer to breaching the skin barrier: An innovative development for amputees. J Anat **209**: 59-67.

Pendegrass CJ, Gordon D, Middleton CA, Man Sun S Ng, Blunn GW (2008). Sealing the skin barrier around transcutaneous implants: *In vitro* study of keratinocyte proliferation and adhesion in response to surface modifications of titanium alloy. J Bone Joint Surg Br **90**: 114-121.

Pendegrass CJ, Middleton CA, Gordon D, Jacob J, Blunn GW (2010). Measuring the strength of dermal fibroblast attachment to functionalised titanium alloys *in vitro*. J Biomed Mater Res A **92**: 1028-1037.

Raisanen L, Kononen M, Juhanoja J, Varpavaara P, Hautaniemi J, Kivilahti J, Hormia M (2000). Expression of cell adhesion complexes in epithelial cells seeded on biomaterial surfaces. J Biomed Mater Res **49**: 79-87.

Shimono M, Ishikawa T, Enokiya Y, Muramatsu T, Matsuzaka KI, Inoue T, Abiko Y, Yamaza T, Kido MA, Tanaka T, Hashimoto S (2003). Biological characteristics of the junctional epithelium. J Electron Microsc (Tokyo) **52**: 627-639.

Shiraiwa M, Goto T, Yoshinari M, Koyano K, Tanaka T (2002). A study of the initial attachment and subsequent behaviour of rat oral epithelial cells cultured on titanium. J Periodontol **73**: 852-860.

Tillander J, Hagberg K, Hagberg L, Branemark R (2010). Osseointegrated titanium implants for limb prostheses attachments: infectious complications. Clin Orthop Relat Res **468**: 2781-2788.

Walko G, Castañón MJ, Wiche G (2014). Molecular architecture and function of the hemidesmosome. Cell Tissue Res [Epub ahead of print] PMID: 25487405.

Editor's Note: All questions/comments by the reviewers were answered by text changes. Therefore, there is no Discussion with Reviewers section.